ACS APPLIED MATERIALS & INTERFACES

Research Article

www.acsami.org

Negative Magnetoresistance in a Vertical Single-Layer Graphene Spin Valve at Room Temperature

Arun Kumar Singh and Jonghwa Eom*

Department of Physics and Graphene Research Institute, Sejong University, Seoul 143-747, Korea

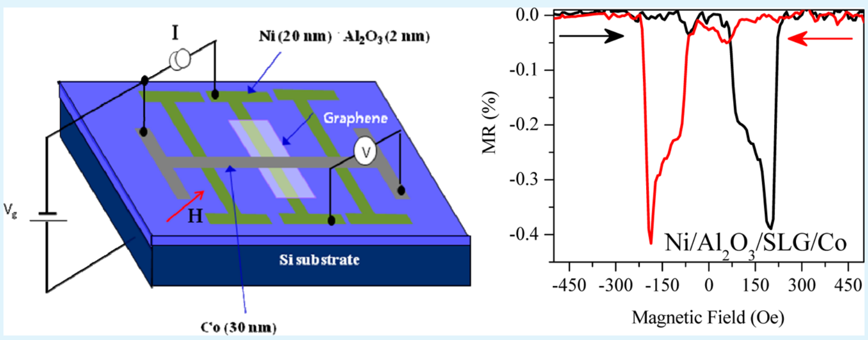

ABSTRACT: Single-layer graphene (SLG) is an ideal material for spintronics because of its high charge-carrier mobility, long spin lifetime resulting from the small spin−orbit coupling, and hyperfine interactions of carbon atoms. Here, we report a vertical spin valve with SLG with device configuration $Co/SLG/Al_2O_3/Ni$. We observed negative magnetoresistance (−0.4%) for the $Co/SLG/Al_2O_3/Ni$ junction at room temperature. However, the $Co/Al_2O_3/Ni$ junction, which is without graphene, shows positive magnetoresistance. The current−voltage ($I-V$) characteristics of both $Co/SLG/Al_2O_3/Ni$ and $Co/Al_2O_3/Ni$ junctions are nonlinear, and this reveals that charge transport occurs by a tunneling mechanism. We have also explained the reason for negative magnetoresistance for the $Co/SLG/Al_2O_3/Ni$ junction.

KEYWORDS: *single-layer graphene, spin valve, magnetoresistance, vertical transport, spintronics*

1. INTRODUCTION

In recent years, spintronics is a rapidly growing field where the spin degree of freedom is manipulated in solid-state devices. Spintronic devices have several advantages over conventional charge-based electronics. They are much smaller in size, more energy efficient, easily controlled by an externally applied magnetic field, and more powerful for certain applications.[1−4] The spin valve is an elementary device to detect spin transport in a material, in which a nonmagnetic medium is contacted by two ferromagnetic electrodes whose electrical resistance depends on the spin state of the electrons passing through the device and so can be controlled by an external magnetic field. Spin transport in graphene draws great attention because of the observation of long spin relaxation lengths (∼2 μm) with relaxation times (∼150 ps) at room temperature (RT) in mechanically exfoliated single-layer graphene (SLG).[5−8] Graphene is a promising material for spintronics because of not only its low intrinsic spin−orbit and hyperfine coupling but also several other advantages such it being single atom ultrathin, highly uniform, and defect-free, and graphene's inert chemical character minimizes the interfacial reaction and interdiffusion, providing well-defined interfaces.[9] It was reported that graphene acts as a tunnel barrier for the current perpendicular-to-plane (CPP) geometry.[10] If graphene is sandwiched between two ferromagnetic metal electrodes, it works as a magnetic tunnel junction (MTJ), which is a basic element of many memory devices nowadays. Nowadays, metal oxides, mainly Al_2O_3 and MgO, have been widely used as tunnel barriers. However, Al_2O_3 and MgO have several problems relating both to various material properties, such as nonuniform thicknesses, pinholes, and defects, that compromise their performance and reliability.[10]

Karpan et al. theoretically predicated that cobalt/graphene/cobalt or nickel/graphene/nickel could be the perfect spin filter because lattice constants of graphene or graphite almost perfectly match with the surface lattice constants of cobalt and nickel.[11,12] The lattice mismatch of nickel is only 1.3% with graphene. Another reason is the absence of majority spin states of nickel and cobalt near the K point of graphene, which allows perfect spin filtering.[12] Recently, several SLG-based spin valves have been made; however, a very small spin signal was detected at RT (300 K). Mohiuddin et al. first reported spin-polarized conduction perpendicular to the plane of the mechanically exfoliated graphene in the CPP geometry at different temperatures.[13] They found that graphene was sufficient to reduce the exchange coupling between the magnetic electrodes, and a magnetoresistance (MR) ratio of about 0.4% was found for NiFe/graphene/NiFe at low temperature (77 K).[13] Cobas et al. recently studied graphene as a tunnel barrier between two ferromagnetic electrodes. They found only 0.25% MR for the

Received: November 4, 2013
Accepted: February 4, 2014
Published: February 4, 2014

device configuration NiFe/graphene/Co/Ti/Au at RT, where SLG was grown by a chemical vapor deposition (CVD) technique.[10] Previously, our group has reported the spin valve of a CVD-grown SLG with the configuration NiFe/graphene/NiFe at different temperatures. We found less than a 0.2% MR ratio for the device NiFe/SLG/NiFe at RT.[14]

In this paper, we report a vertical spin valve that employs mechanically exfoliated SLG inserted between two ferromagnets with the device configuration Co/SLG/Al_2O_3/Ni. The SLG film is confirmed using optical microscopy and Raman spectroscopy. We observed negative MR (−0.4%) for the Co/SLG/Al_2O_3/Ni junction, which is higher than those at RT reported in previous papers. However, the Co/Al_2O_3/Ni junction, which is without graphene, shows positive MR. The current−voltage (I−V) characteristics of both the Co/SLG/Al_2O_3/Ni and Co/Al_2O_3/Ni junctions are nonlinear, and this revealed that charge transport occurs by a tunneling mechanism. We have also explained the reason for negative MR for the Co/SLG/Al_2O_3/Ni junction.

2. EXPERIMENTAL SECTION

Figure 1a shows a schematic illustration of our vertical spin-valve device structure. The current is applied through graphene layers from a

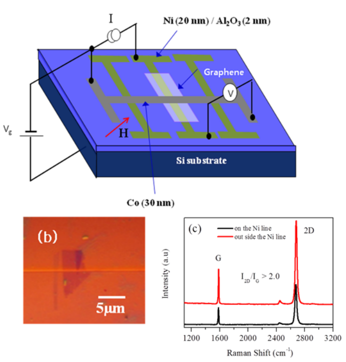

Figure 1. (a) Schematic diagram of the vertical graphene spin valve consisting of (bottom) Ni/Al_2O_3, (top) a cobalt ferromagnetic electrode, and mechanically exfoliated SLG in between the ferromagnetic electrodes. The measurement configuration is also shown, and the magnetic field is applied at 45° to the direction of the ferromagnetic electrodes. (b) Optical image of the SLG on prepatterned Al_2O_3/Ni lines. (c) Raman spectra for the SLG on Al_2O_3/Ni lines and a SiO_2 substrate.

ferromagnet in the CPP structure and detected by another ferromagnet. The magnetic field is applied at 45° to the direction of the ferromagnetic electrodes, as shown in Figure 1a. The big patterned electrodes (Cr/Au of 5/10 nm) were made by photolithography on a Si/SiO_2 substrate, and Ni lines (thickness 20 nm) of width 0.5 μm were made by e-beam lithography. Subsequently, aluminum of 2 nm was deposited over a nickel electrode without breaking the vacuum and oxidized in an O_2 atmosphere for 2 h. The SLG was prepared by mechanical exfoliation of natural graphite flakes using scotch tape and then transferred onto a spin-coated polymer layer consisting of poly(methyl methacrylate) (PMMA; molecular weight 950K) on top of a water-soluble layer, poly(vinyl alcohol) (PVA), followed by a SiO_2/Si substrate. After identification of a suitable flake by optical microscopy, deionized water was used to dissolve the bottom PVA layer and PMMA, with graphene floating on top of the water bath. Graphene with a PMMA layer was transferred onto a poly(dimethylsiloxane) (PDMS) film (thickness ~1 mm). SLG/PMMA/PDMS was inverted and clamped onto the micromanipulator mounted on an optical microscope. The micromanipulator and optical microscope were used to align the graphene on prepatterned electrodes. PDMS was removed from SLG/PMMA/PDMS by heating the substrate at 80 °C for 5 min, and PMMA was then removed by immersion in acetone for 1 day. The SLG was transferred onto prepatterned Al_2O_3/Ni lines, as shown in Figure 1b. Subsequently, Co electrode (thickness 30 nm) of width 0.5 μm was patterned over SLG/Ni by using e-beam lithography and lift-off process. Raman spectra were carried out at RT with Renishaw microspectrometer over wave number from 1100 to 3200 cm^{-1} with the laser wavelength of 514 nm. The four probe electrical measurements of our spin valve device were carried out using lock-in amplifier at RT.

3. RESULTS AND DISCUSSION

The mechanically exfoliated SLG is confirmed by optical microscopy and Raman spectroscopy. The optical image of SLG on the prepatterned Ni/Al_2O_3 line is shown in Figure 1b. Figure 1c shows the Raman spectra of the SLG on a SiO_2 substrate and Ni line; however, not significant differences have been observed in the Raman spectra of the SLG on a SiO_2 substrate and Ni line. The characteristic G and 2D peaks for the SLG appears around 1582 and 2673 cm^{-1}, respectively. The intensity ratio of I_{2D}/I_G is greater than 2, and a full width at half-maximum (FWHM) of the 2D band of about 30 cm^{-1} is the signature of the SLG. For the SLG intensity of the 2D peak must be 2 times greater than the intensity of the G peak. The shape of the 2D peak and ratio of the intensity between the G and 2D peaks are used to discriminate the SLG from a multilayered graphene.[15−17] The absence of the D peak in the SLG is an indication of a defect-free high-quality graphene, and there is no damage of the SLG after transfer on the prepatterned Ni/Al_2O_3 line. The devices with graphene and without a graphene spin valve were simultaneously made on the same substrate, and the schematic diagram is shown in Figure 1a for both devices with or without graphene.

Figure 2a shows an optical micrograph of a SLG stack vertical spin valve with a junction area of 0.5 × 0.5 μm^2. The MR data

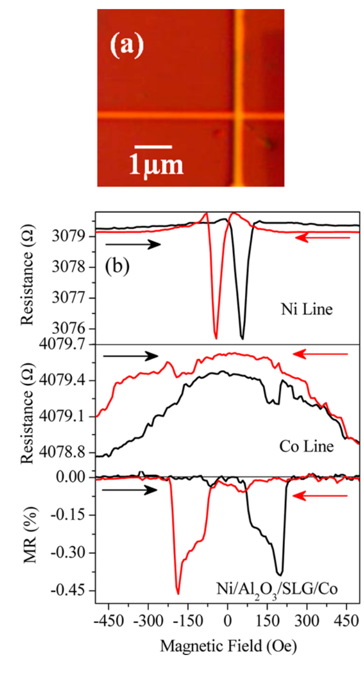

Figure 2. (a) Optical image of a Co/SLG/Al_2O_3/Ni device. (b) MR versus magnetic field graph for Al_2O_3/Ni lines and Co lines and MR for a vertical SLG spin valve (Co/SLG/Al_2O_3/Ni) at RT. The arrows indicate the direction of the MR trace.

for Al_2O_3/Ni line, Co line, and Co/SLG/Al_2O_3/Ni are shown in Figure 2b. The MR data were measured by a lock-in amplifier by applying a constant current through one bottom electrode and one top electrode, and another pair of electrodes was used to measure the voltage drop. A magnetic field (H) was applied in-plane at 45° to the direction of the ferromagnetic electrodes in MR measurements. The magnetization of nickel and cobalt electrodes was reversed at a magnetic field corresponding to their respective coercivities. The switching field of a nickel ferromagnetic electrode is much lower (~75 Oe) than the cobalt ferromagnetic electrode (~150−200 Oe), as shown in Figure 2b. Thus, their magnetization can be aligned either parallel or antiparallel, and two distinct resistance states are observed in magneto transport measurements. The MR ratio of the junction Co/SLG/Al_2O_3/Ni is found to be ~−0.4%. The MR ratio can be defined as MR = $(R_{AP} - R_P)/R_P$, where R_P is the resistance corresponding to the parallel and R_{AP} is the resistance corresponding to the antiparallel alignment of magnetization. We observed negative MR for the Co/SLG/Al_2O_3/Ni junction, and it is consistent among different runs. We never observed positive MR for the Co/SLG/Al_2O_3/Ni junction. Theoretically, a 25% MR ratio of a perfectly ordered single-crystal Ni(111)/graphene/Ni(111) junction in the CPP structure was predicted.[12] However, this value drops drastically if the nickel layer contains disorder or roughness adjacent to the SLG.[12]

We measured a negative MR ratio of 0.4% for the Co/SLG/Al_2O_3/Ni junction at RT. Dlubak et al. observed higher MR at low temperature (1.4 K) of the same device structure; the higher MR of their device may be due to the larger device area.[20] The lower MR ratio in comparison to that in theoretical prediction may be due to disorder or roughness at both graphene/metal interfaces. However, this value is higher than other reported values at RT.[10,13,14] For comparison, we also measured the MR for the Co/Al_2O_3/Ni junction, as shown in Figure 3a. The MR for the Co/Al_2O_3/Ni junction is found to be positive, and this is consistent with previously reported papers.[18−20] It is already reported that the spin polarizations of both the Co/Al_2O_3 and Ni/Al_2O_3 junctions are positive.[20−22] Therefore, the Co/Al_2O_3/Ni junction shows positive MR. The I−V characteristics at RT for the Co/SLG/Al_2O_3/Ni and Co/Al_2O_3/Ni junctions are shown in Figure 3b. The I−V characteristics of junctions were measured by four-probe geometry. The nonlinear and symmetric curves of both junctions revealed that charge transport across the SLG occurs by a tunneling mechanism.

Figure 4 shows the phenomenological representation of positive spin signals for Co/Al_2O_3/Ni (without graphene) and negative spin signals for Co/SLG/Al_2O_3/Ni (with SLG). Negative MR was previously reported for organic semiconductors.[23−26] The spin reversal observed at the Co/SLG/Al_2O_3/Ni junction is due to the presence of a graphene layer between Al_2O_3/Ni and Co ferromagnet electrodes. Karpan et al. predicated by using ab initio calculations and claimed that the CPP structure of the ferromagnet/graphene/ferromagnet junction works as a perfect spin filter, where ferromagnetic electrodes are close-packed surfaces of cobalt or nickel.[12] They have explained their results using Fermi surface projections of graphene, nickel, and cobalt. They have found that there are no majority spin states for nickel and cobalt close to the K point, whereas minority spin states exist everywhere in the Brillouin zone. Therefore, only minority spins have a continuous transport channel through the graphene to the ferromagnetic electrode, while majority spins have no direct conduction path. This may be the reason for spin reversal of the Co/SLG/Al_2O_3/Ni junction.

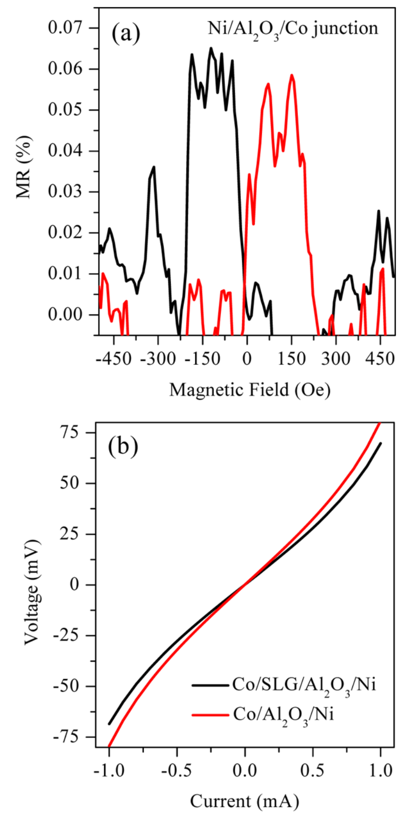

Figure 3. (a) MR for Co/Al_2O_3/Ni (without graphene) device at RT. (b) I−V curve for devices Co/SLG/Al_2O_3/Ni and Co/Al_2O_3/Ni.

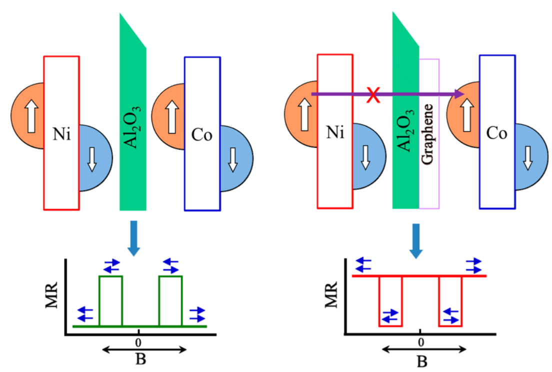

Figure 4. Systematic representation of the positive and negative spin signals: positive spin signal for Co/Al_2O_3/Ni (without graphene) shown on the left side, and negative spin signal for Co/SLG/Al_2O_3/Ni (with SLG) shown on the right side.

4. CONCLUSIONS

We report negative MR for a mechanically exfoliated SLG vertical spin valve with the device configuration Co/SLG/Al_2O_3/Ni. The SLG film is confirmed by using optical microscopy and Raman spectroscopy. We observed negative MR (−0.4%) of the Co/SLG/Al_2O_3/Ni junction, which is higher than those reported in previous papers at RT. However, the Co/Al_2O_3/Ni junction, which is without graphene, shows positive MR. The I−V characteristics of both the Co/SLG/Al_2O_3/Ni and Co/Al_2O_3/Ni junctions revealed that charge transport occurs by a tunneling mechanism. We have also explained the reason for negative MR for the Co/SLG/Al_2O_3/Ni junction. Our study may be useful for future graphene-based spintronics devices.

AUTHOR INFORMATION

Corresponding Author

*E-mail: eom@sejong.ac.kr.

Notes

The authors declare no competing financial interest.

ACKNOWLEDGMENTS

This research was supported by the Nano-Material Technology Development Program (Grant 2012M3A7B4049888) and the Converging Research Center Program (Grant 2013K000172) through the National Research Foundation of Korea (NRF) funded by the Ministry of Science, ICT, and Future Planning. This research was also supported by the Basic Science Research Program (Grants 2010-0020207 and 2013R1A1A2061396) through the NRF funded by the Ministry of Education.

REFERENCES

(1) Žutic, I.; Jaroslav, F.; Das Sarma, S. *Rev. Mod. Phys.* **2004**, *76*, 323−410.

(2) Wolf, S. A.; Awschalom, D. D.; Buhrman, R. A.; Daughton, J. M.; Molnár, S. V.; Roukes, M. L.; Chtchelkanova, A. Y.; Treger, D. M. *Science* **2001**, *294*, 1488−1495.

(3) Behin-Aein, B.; Datta, D.; Salahuddin, S.; Datta, S. *Nat. Nanotechnol.* **2010**, *5*, 266−270.

(4) Johnson, M.; Silsbee, R. H. *Phys. Rev. Lett.* **1985**, *55*, 1790−1793.

(5) Tombros, N.; Józsa, C.; Popinciuc, M.; Jonkman, H. T.; van Wees, B. J. *Nature* **2007**, *448*, 571−574.

(6) Maassen, T.; van den Berg, J. J.; IJbema, N.; Fromm, F.; Seyller, T.; Rositza, Y.; van Wees, B. J. *Nano Lett.* **2012**, *12*, 1498−1502.

(7) Guimarães, M. H. D.; Veligura, A.; Zomer, P. J.; Maassen, T.; Vera-Marun, I. J.; Tombros, N.; van Wees, B. J. *Nano Lett.* **2012**, *12*, 3512−3517.

(8) Han, W.; Pi, K.; Bao, W.; McCreary, K. M.; Li, Y.; Wang, W. H.; Lau, C. N.; Kawakami, R. K. *Appl. Phys. Lett.* **2009**, *94*, 222109.

(9) Chen, J. J.; Meng, J.; Zhou, Y. B.; Wu, H. C.; Bie, Y. Q.; Liao, Z. M.; Yu, D. P. *Nat. Commun.* **2013**, *4*, 1921.

(10) Cobas, E.; Friedman, A. L.; van't Erve, O. M. J.; Robinson, J. T.; Jonker, B. T. *Nano Lett.* **2012**, *12*, 3000−3004.

(11) Karpan, V. M.; Giovanetti, G.; Khomyakov, P. A.; Talanana, M.; Starikov, A. A.; Zwierzycki, M.; van den Brink, J.; Brocks, G.; Kelly, P. J. *Phys. Rev. Lett.* **2007**, *99*, 176602.

(12) Karpan, V. M.; Khomyakov, P. A.; Starikov, A. A.; Giovannetti, G.; Zwierzycki, M.; Talanana, M.; Brocks, G.; van den Brink, J.; Kelly, P. J. *Phys. Rev. B* **2008**, *78*, 195419.

(13) Mohiuddin, T. M. G.; Hill, E.; Elias, D.; Zhukov, A.; Novoselov, K.; Geim, A. *IEEE Trans. Magn.* **2008**, *44*, 2624−2627.

(14) Iqbal, M. Z.; Iqbal, M. W.; Lee, J. H.; Kim, Y. S.; Chun, S. H.; Eom, J. *Nano Res.* **2013**, *6*, 373−380.

(15) Ferreira, E. H. M.; Moutinho, M. V. O.; Stavale, F.; Lucchese, M. M.; Capaz, R. B.; Achete, C. A.; Jorio, A. *Phys. Rev. B* **2010**, *82*, 125429.

(16) Ferrari, A. C. *Solid State Commun.* **2007**, *143*, 47−57.

(17) Singh, A. K.; Ahmad, M.; Singh, V. K.; Shin, K.; Seo, Y.; Eom, J. *ACS Appl. Mater. Interfaces* **2013**, *5*, 5276−5281.

(18) Miyazaki, T.; Tezuka, N. *J. Magn. Magn. Mater.* **1995**, *151*, 403−410.

(19) Suezawa, Y.; Takahashi, F.; Gondo, Y. *Jpn. J. Appl. Phys.* **1992**, *31*, L1415−L1416.

(20) Dlubak, B.; Martin, M. B.; Weatherup, R. S.; Yang, H.; Deranlot, C.; Blume, R.; Schloegl, R.; Fert, A.; Anane, A.; Hofmann, S.; Seneor, P.; Robertson, J. *ACS Nano* **2012**, *6*, 10930−10934.

(21) Monsma, D. J.; Parkin, S. S. P. *Appl. Phys. Lett.* **2000**, *77*, 883.

(22) Miao, G.-X.; Münzenberg, M.; Moodera, J. S. *Rep. Prog. Phys.* **2011**, *74*, 036501.

(23) Gu, H.; Zhang, X.; Wei, H.; Huang, Y.; Wei, S.; Guo, Z. *Chem. Soc. Rev.* **2013**, *42*, 5907−5943.

(24) Li, F. *ACS Appl. Mater. Interfaces* **2013**, *5*, 8099−8104.

(25) Ruden, P. *Nat. Mater.* **2011**, *10*, 8−9.

(26) Ehrenfreund, E.; Vardeny, Z. V. *Phys. Chem. Chem. Phys.* **2013**, *15*, 7967−7975.